Modelling isothermal fission gas release

P. van Uffelen

SCK•CEN,
Mol, Belgium

Abstract. The present paper presents a new fission gas release model consisting of two coupled modules. The first module treats the behaviour of the fission gas atoms in spherical grains with a distribution of grain sizes. This module considers single atom diffusion, trapping and fission induced re-solution of gas atoms associated with intragranular bubbles, and re-solution from the grain boundary into a few layers adjacent to the grain face. The second module considers the transport of the fission gas atoms along the grain boundaries. Four mechanisms are incorporated: diffusion controlled precipitation of gas atoms into bubbles, grain boundary bubble sweeping, re-solution of gas atoms into the adjacent grains and gas flow through open porosity when grain boundary bubbles are interconnected. The interconnection of the intergranular bubbles is affected both by the fraction of the grain face occupied by the cavities and by the balance between the bubble internal pressure and the hydrostatic pressure surrounding the bubbles. The model is under validation. In a first step, some numerical routines have been tested by means of analytic solutions. In a second step, the fission gas release model has been coupled with the FTEMP2 code of the Halden Reactor Project for the temperature distribution in the pellets. A parametric study of some steady-state irradiations and one power ramp have been simulated successfully. In particular, the Halden threshold for fission gas release and two simplified FUMEX cases have been computed and are summarised.

1. INTRODUCTION

Economics and prudent utilisation of natural resources have provided strong incentives for extending the average discharge burnup levels of light water reactor (LWR) fuel in commercial power plants. This might have implications for fuel integrity and, accordingly, this could be in conflict with safety requirements. One of the issues of primary interest in high burnup fuel is the behaviour of the fission gas atoms. In addition to the build-up of the rod internal pressure, the release of volatile and inert gas atoms could impede the heat transfer between the cladding and the pellets. On the other hand, gas atoms remaining in the pellets engender swelling which in turn can boost the mechanical interaction between the pellets and the cladding at high burnup. It is therefore essential to be able to predict the amount of gas produced and released during operation, especially at high burnup where the release is expected to increase [[1], [2].

From the FUMEX exercise [3], it appeared that difficulties still remain with modelling fission gas release. It has been recognised that being a highly non-linear process, strongly influenced by temperature and feedback effects, accurate modelling is difficult over the whole range of release values from 0 to 100%. In particular, the region around 1% is extremely difficult to predict accurately and this just happens to be the most important region above which gas release and rod internal pressure can run away. Although there is available the empirical Halden criterion relating fuel central temperature to burnup at which 1% release can be exceeded, there is a need for elucidating the underlying mechanisms in order to refine the kinetics of release in this region. This constitutes the driving force for our attempt at developing an improved mechanistic model for fission gas release (FGR) in LWR fuel.

In a first step towards modelling FGR, the different mechanisms have been recapitulated in an internal document [4]. In a second step, an overview was made of the relevant models from which a first proposal was made in order to reconcile two contradictory approaches to the

behaviour of fission gases at the grain boundaries [5]: some people favour the grain boundary diffusion mechanism [6][7][8], while others advocate that fission products only accumulate in the grain boundary bubbles until saturation occurs, entailing the opening of the tunnel network along grain edges and the venting of the bubbles [9][10][11][12][13][14][15]. Both points of view could be reconciled as follows: grain boundary diffusion in presence of grain boundary traps is operative at low burnup values while there is a switch to nucleation and growth of grain boundary bubbles in controlling intergranular fission gas atom motion under certain conditions. In order to asses this switch, we assessed the mean distance travelled by a gas atom at the grain boundary before being swallowed up by an intergranular trap [16]. It was concluded that the contribution of grain boundary diffusion to fission gas release on the pellet scale is strongly inhibited as soon as the aerial coverage of the grain boundary traps is about 1% and the trap density exceeds 0.1 μm^{-2}. Consequently we have proposed a simplified or alternative model for the intergranular behaviour of fission products.

In the following section, we describe the resulting mechanistic model for FGR and the concomitant gaseous swelling in LWR fuel. The model is related to the model of Kogai [17], in which we have implemented several modifications, among which a new description of fission product precipitation in grain boundaries [18] and fission induced resolution effects.

The model is under validation. In a first step, some numerical routines have been tested by means of analytic solutions. In the second step of the validation, the fission gas release model has been coupled with the FTEMP2 code [19] of the Halden Reactor Project for the temperature distribution in the pellets, as summarised in the third section of the present paper. A parametric study of some steady-state irradiations and one power ramp have been simulated successfully. In particular, the Halden threshold for fission gas release and two simplified FUMEX [3] cases have been computed and are presented in the fourth section. Finally, in the last section we draw the conclusions of the present computations and sketch the future work on the model for fission gas release.

2. MODEL DESCRIPTION

The model treats the migration of the fission gas atoms in two coupled phases.

2.1. Intragranular Module

The first phase of the FGR model deals with the transport of the fission products in spherical grains with a distribution of grain sizes [20] in order to avoid overprediction of the released fraction [6]. Three mechanisms are incorporated in this part: single atom diffusion in the bulk of the fuel matrix, trapping and resolution associated with intragranular bubbles, and resolution of fission products from grain boundary bubbles into a resolution layer adjacent to the grain face:

$$\frac{\partial C_v(r,t)}{\partial t} = D_{eff}\Delta C_v(r,t) + S_v(r,t) \tag{1}$$

where

$$D_{eff} = \frac{b}{b+g} D_v \tag{2}$$

The single atom diffusion coefficient (D_v) given by Kogai [17] has been applied. The trapping (g) and resolution (b) associated with the intragranular bubbles [21][22] are taken into account by means of an effective diffusion coefficient (D_{eff}) [23], which is only valid when the bubbles are considered to be saturated [24].

The resolution of fission products accumulated at the grain boundary [25][26], introduces a supplementary source term (S_{res}) into a few layers adjacent to the grain face:

$$S_v(r,t) = \begin{cases} Y_{FP}\dot{F} & 0 \le r \le R_{grain} - 2\delta_R \\ Y_{FP}\dot{F} + S_{res} & R_{grain} - 2\delta_R \le r \le R_{grain} \end{cases} \tag{3}$$

The supplementary source term has been incorporated by means of the smeared model [27]:

$$S_{res} = B_{gb} \frac{3R_{grain}^3 \delta_{gb}}{2\delta_R\left(3R_{grain}^2 - 3R_{grain}\delta_R + \delta_R^2\right)}\left(C_{gbv} + C_{gbb}\right) \tag{4}$$

where the grain boundary concentrations (C_{gbv} and C_{gbb}) are determined by the intergranular module of the FGR model.

2.2. Intergranular Module

In the second phase of the model, we consider the transport of the fission gas atoms along the grain boundaries in presence of secondary phases and grain face bubbles [16]. The gas atoms are considered to exist in two phases at the grain boundary: one fraction is dissolved in the grain boundary volume (C_{gbv}) whereas the other part is accumulated in bubbles (C_{gbb}). Four mechanisms are incorporated: diffusion controlled precipitation of gas atoms into bubbles [18], grain boundary bubble sweeping associated to bubble growth, re-solution of gas atoms into the adjacent grains and gas flow through open porosity when grain boundary bubbles are interconnected [17]. This results in a coupled system of 3 ordinary differential equations:

$$\begin{cases} \dfrac{\partial \rho_{bl}}{\partial t} = \dfrac{\delta_{gb} D_m^v \Omega}{4 f(\theta) \rho_{bl}^2 kT}\left(P_{bl} - P_h - \dfrac{2\gamma}{\rho_{bl}}\right) k \\ \dfrac{\partial \hat{C}_{gbv}}{\partial t} = (1-\phi) J_1 - J_2' - J_2'' - J_3' \\ \dfrac{\partial \hat{C}_{gbb}}{\partial t} = \phi J_1 + J_2' + J_2'' - J_3'' - J_4 \end{cases} \tag{5}$$

where the aerial fraction occupied by the grain boundary bubbles (ϕ) is given by

$$\phi = \begin{cases} \pi R_{bl}^2 C_{bl}^0 & R_{bl} < R_{bl}^* \\ \dfrac{\pi}{4} & R_{bl} \ge R_{bl}^* \end{cases} \tag{6}$$

The radius at which grain boundary bubble interconnect (R_{bl}^{*}) is determined by the initial grain boundary bubble density:

$$R_{bl}^{*} = \frac{1}{2\sqrt{C_{bl}^{0}}} \tag{7}$$

The grain boundary concentrations C_{gbv} and C_{gbb} per unit of volume of the grain boundary are converted to the quantities $\hat{C}_{gbv}$ and $\hat{C}_{gbb}$ respectively, in order to express them per unit volume of the macroscopic solid:

$$\begin{aligned} \hat{C}_{\mathrm{gbv}} &= C_{gbv}\delta_{gb}S_{gb} \\ \hat{C}_{\mathrm{gbb}} &= C_{gbb}\delta_{gb}S_{gb} \end{aligned} \tag{8}$$

In the following sections we will formulate the different terms in (5) explicitly.

2.2.1. The intergranular source term

J_1 represents the average outcoming flux of a distribution of grains and is coupled to the intragranular module of the FGR model:

$$J_1 = \sum_{k,l} N_{klm} \cdot 2\left[-\frac{4\pi R_{klm}^{2}}{2} D_{v,klm} \left.\frac{\partial\left(C_{v,klm}\right)}{\partial r}\right|_{r=R_{klm}} \right] \tag{9}$$

where the term between brackets represents the outcoming flux of fission products from a grain with indices *k,l,m*. The factor 2 in front of the brackets in the right hand side of (9) accounts for the fact that fission products flow to or from both sides of a grain boundary.

2.2.2. Diffusion controlled precipitation of fission gas atoms

The flux J'_2 represents the flow of gas atoms dissolved in the grain boundary volume to the intergranular bubbles by diffusive capture [18]:

$$J_2' = \left[\frac{8D_{gb}\phi(1-\phi)^{2}}{(1-\phi)(\phi-3)-2\ln(\phi)} \right] \frac{\hat{C}_{gbv}}{R_{bl}^{2}} \tag{10}$$

2.2.3. Grain boundary bubble sweeping

In deriving the expression for the capture rate constant for the flux of gas atoms precipitating in intergranular bubbles, we have neglected bubble growth. In order to account for the growth of the grain boundary bubbles, we introduce a supplementary flux term (J_2'') of fission gas atoms dissolved in the grain boundary to the intergranular bubbles by bubble sweeping:

$$J_2'' = \begin{cases} 2\pi \dfrac{\phi}{\rho_{bl}} \dfrac{d\rho_{bl}}{dt} \hat{C}_{gbv} & \dfrac{d\rho_{bl}}{dt} > 0 \\ 0 & \dfrac{d\rho_{bl}}{dt} \le 0 \end{cases} \tag{11}$$

2.2.4. Fission induced re-solution at grain boundaries

The fission spikes can redissolve a fraction of the fission gas atoms accumulated in the grain boundary into the adjacent grains. The rate at which this occurs is determined by the re-solution rate coefficient (B_{gb}) which in turn is dependent on the fission rate density ($\dot{F}$). The resulting flux of gas atoms leaving the grain boundary (thereby opposing the outcoming diffusive flux J_1) reads:

$$J_3 = J_3' + J_3'' = B_{gb}\left(\hat{C}_{gbv} + \hat{C}_{gbb}\right) \tag{12}$$

where

$$B_{gb} = B_{gb}^{*}\frac{\dot{F}}{\dot{F}^{ref}} \tag{13}$$

and the reference fission rate density ($\dot{F}^{ref}$) is taken at a linear heat rate of 20kW/m.

2.2.5. Gas flow through the interconnected tunnel network

When the grain boundary bubbles reach a critical size (R_{bl}^{*}), they interconnect and vent their content to the free volume of the rod. This release by gaseous flow trough the tunnel network of interconnected grain boundary bubbles, cracks and open porosity is incorporated in J_4. The additional flux term is derived from the equation of Poiseuille in a capillary tube [17][28]:

$$J_4 = \frac{V_t P_{bl}^2 N_{bl} S_{gb}}{\eta kT} \tag{14}$$

where

$$\eta = \frac{1}{\pi\zeta^2 N_A}\sqrt{\frac{MRT}{\pi}} \cong 26.69\frac{\sqrt{MT}}{\zeta^2} \tag{15}$$

$$V_t = V_t^0 f(\phi) g(\sigma_e) \tag{16}$$

$$V_t^0 = \frac{\pi a^4}{8L} \tag{17}$$

$$\sigma_e = \frac{P_h + \phi P_{bl}}{1-\phi} \tag{18}$$

$$f(\phi) = 1 - \exp\left[1 - \left(\frac{\phi}{\phi^*}\right)^{10}\right] \tag{19}$$

$$g(\sigma_e) = 1 - \exp\left[1 - \left(\frac{\sigma_e}{\sigma_e^*}\right)^{10}\right] \tag{20}$$

The interconnection of the intergranular bubbles is thus affected both by the fraction of the grain face occupied by the cavities (ϕ) and by the balance between the bubble internal pressure (P_{bl}) and the hydrostatic pressure surrounding the bubbles (P_h).

2.2.6. Grain boundary bubble growth

Once the grain boundary bubbles are nucleated, they can growth (or shrink) by means of a vacancy flow along the grain boundary. The balance between the bubble internal pressure, the hydrostatic pressure and the surface tension constitutes the driving force for the growth or shrinkage of the bubbles [29]. The expression for the growth of the lenticular intergranular bubbles is based on the model for void growth on grain boundaries presented by Speight et al. [30]. Yang et al. [31] have verified this model by means of small angle neutron scattering. Matthews et al. [32] and Hayns et al. [33] have extended the idea of Speight et al. by considering gas filled bubbles rather than voids. To include the presence of gas within the cavity, they simply included the gas pressure (P_{bl}) into the chemical potential of the cavity:

$$\frac{\partial \rho_{bl}}{\partial t} = \frac{\delta_{gb} D_m^v \Omega}{4 f(\theta) \rho_{bl}^2 kT} \left(P_{bl} - P_h - \frac{2\gamma}{\rho_{bl}} \right) k(\phi) \tag{21}$$

where

$$k(\phi) = \frac{8(1-\phi)}{(\phi-1)(3-\phi) - 2\ln(\phi)} \tag{22}$$

Matthews et al. have compared their results on swelling in nuclear fuel successfully with the experimental data of Zimmermann [34]. Kashibe et al. [29] confirmed these findings more recently.

3. MODEL APPLICATION

Proper testing of a fission gas release model requires coupling with a general fuel performance code in view of the interrelationship with other phenomena. In a first step, we used the FTEMP2 code [19] from the Halden Reactor Project to assess the radial temperature distribution in the pellets. More precisely, we assume a parabolic temperature distribution in the pellet:

$$T(r) = T_s + (T_c - T_s) \left[1 - \left(\frac{r}{R_{pellet}} \right)^2 \right] \tag{23}$$

where the central temperature (T_c) and the surface temperature (T_s) are provided by FTEMP2. A further simplification in the analysis comes from the normalised fission rate distribution in the pellets ($\dot{f}$) which was taken to be independent of burnup:

$$\dot{f}(x) = \frac{F_1(x)}{\int_0^1 F_1(x) x dx} = \frac{\dot{F}(x)}{\dot{F}_{avg}} \tag{24}$$

where

$$F_1(x) = 1 + 0.4x^4 \tag{25}$$

$$x = \frac{r}{R_{pellet}} \tag{26}$$

and $\dot{F}_{avg}$ corresponds to the pellet averaged fission rate density.

3.1. Simulation of the Threshold For Fission Gas Release

3.1.1. Test procedure

We simulate the (Halden) threshold for the onset of fission gas release, that is we determine the central temperature in the rod and the average burnup in the pellet when the fraction of the released gases reaches 1% during an irradiation at constant linear heat rate (25 kW/m, 30 kW/m, 35 kW/m, and 38 kW/m). We assess the effect of the average grain size (5 μm ≤ R_{grain} ≤ 11.25 μm), the resolution rate constant for fission gas atoms at the grain boundaries at 20kW/m (10^{-5} s^{-1} ≤ B^*_{gb} ≤ 10^{-6} s^{-1} [21][23][27]), the effect of the hydrostatic pressure (P_h) and the grain boundary surface energy (0.7 J/m^2 ≤ γ ≤ 1 J/m^2 [17][21]) on the fission gas release.

3.1.2. Results and discussion

The effects of the parameters under consideration are summarised in Fig. 1, 2, 3 and 4. In the discussion we should bear in mind that the Halden threshold corresponds to a correlation between small and large gas releases -- taken to be 0.5% to 2% -- with the peak fuel centre temperature. This should be kept in mind when comparing our results for a single pellet (i.e. we consider a uniform axial power profile) with that of a whole fuel rod. In view of this our results are very satisfactory and reflect the decline of the release threshold at high burnup [35][36][37].

FIG. 1 reveals the substantial role played by the hydrostatic pressure. According to our model, increasing the hydrostatic pressure leads to a shift of the onset for fission gas release to a higher burnup. These results are in accordance with several observations, both from in-pile and out-of-pile experiments [12][13][29][34][38][39]. Precise knowledge of the hydrostatic stress in the pellet therefore appears to be a prerequisite for the calibration of a fission gas release model.

The effect of the surface energy of the grain face bubbles is very small as expected (FIG. 2). The effect of the grain size on the fission gas release has two different aspects. First, the onset of fission gas release is unaffected by the grain size. This stems from the increase of the specific surface of the grains which is inversely proportional to the grain size alike the amount of gas reaching the grain boundaries by diffusion. The onset of fission gas release corresponds to a certain concentration of the grain boundaries at which saturation occurs with the subsequent venting of the bubbles through an interconnected tunnel network of bubbles. In the present calculations, this saturation concentration is in the order of $2x10^{15}$ atoms/cm^2 which corresponds quite well with other data in the literature [9][40]. According to the results in FIG. 3, there is a slight shift of the burnup where 1% of the fission gases are vented. This can be understood from FIG. 5, where the released fraction is shown as a function of the burnup at a constant linear heat rate of 38 kW/m for three different grain radii. FIG. 5 reveals that the onset of fission gas release, which starts in the pellet centre, is not dependent on the grain size. However, the release after the opening of the tunnel network is diffusion controlled hence it is

increasing with decreasing grain size. The incubation period after which 1% average fission gas release in the pellet is reached, therefore depends slightly on the grain size.

The effect of the resolution rate constant (B^*_{gb}) is significant in the present model, as illustrated in FIG. 4. The effect of the rate constant becomes more perceptible at higher burnups. The results indicate that a value for B^*_{gb} in the order of 10^{-5} s^{-1} provides a good fit. This is in good agreement with 1.55 s^{-1} used by Denis et al [23].

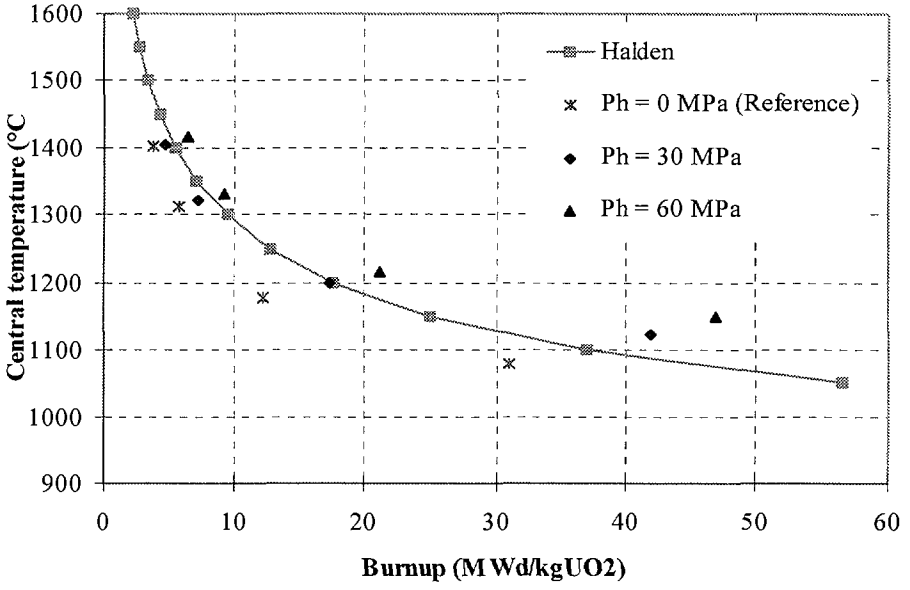

FIG. 1: The effect of the hydrostatic pressure on the central temperature for 1% average fission gas release versus burnup during irradiation at constant linear heat rate.

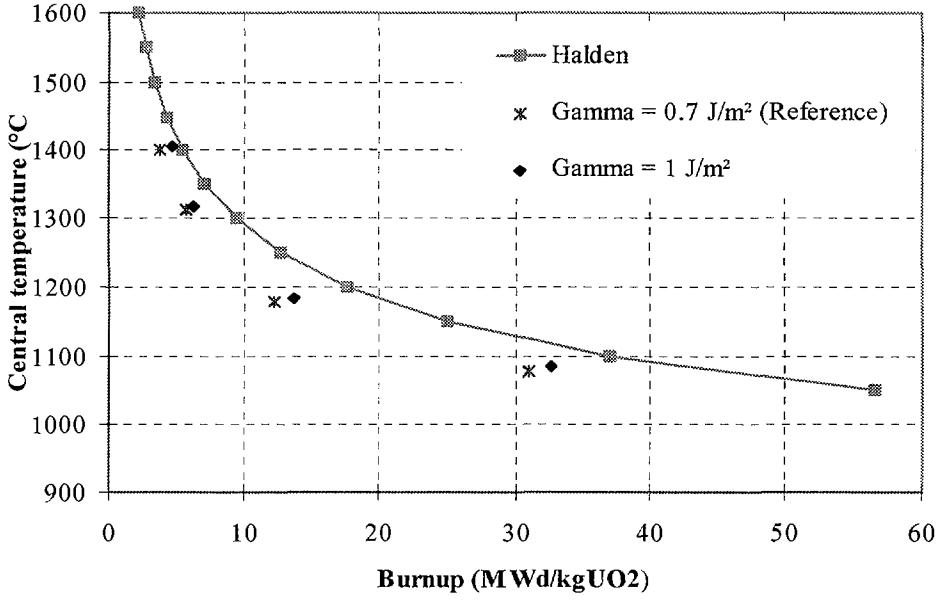

FIG. 2: The effect of the surface energy of intergranular bubbles (gamma) on the central temperature for 1% average fission gas release versus burnup during irradiation at constant linear heat rate.

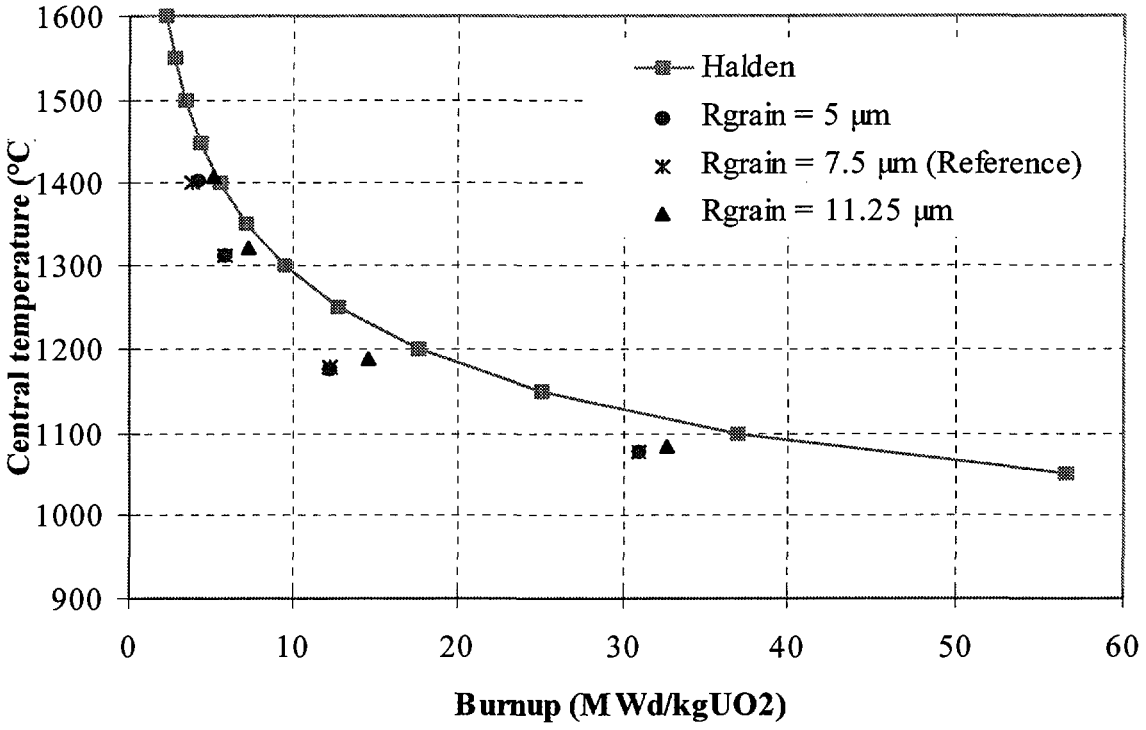

FIG. 3: The effect of the average grain radius on the central temperature for 1% average fission gas release versus burnup during irradiation at constant linear heat rate.

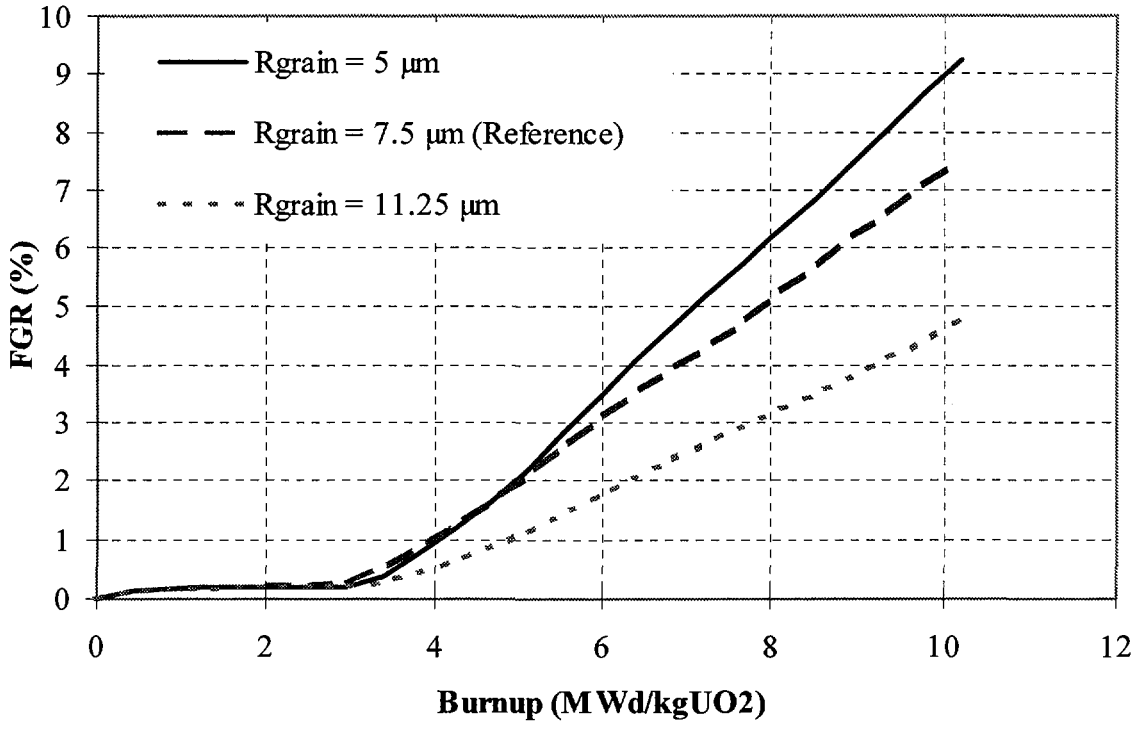

FIG. 4: The fission gas release rate at 38 kW/m as a function of the average burnup for three different average grain radii.

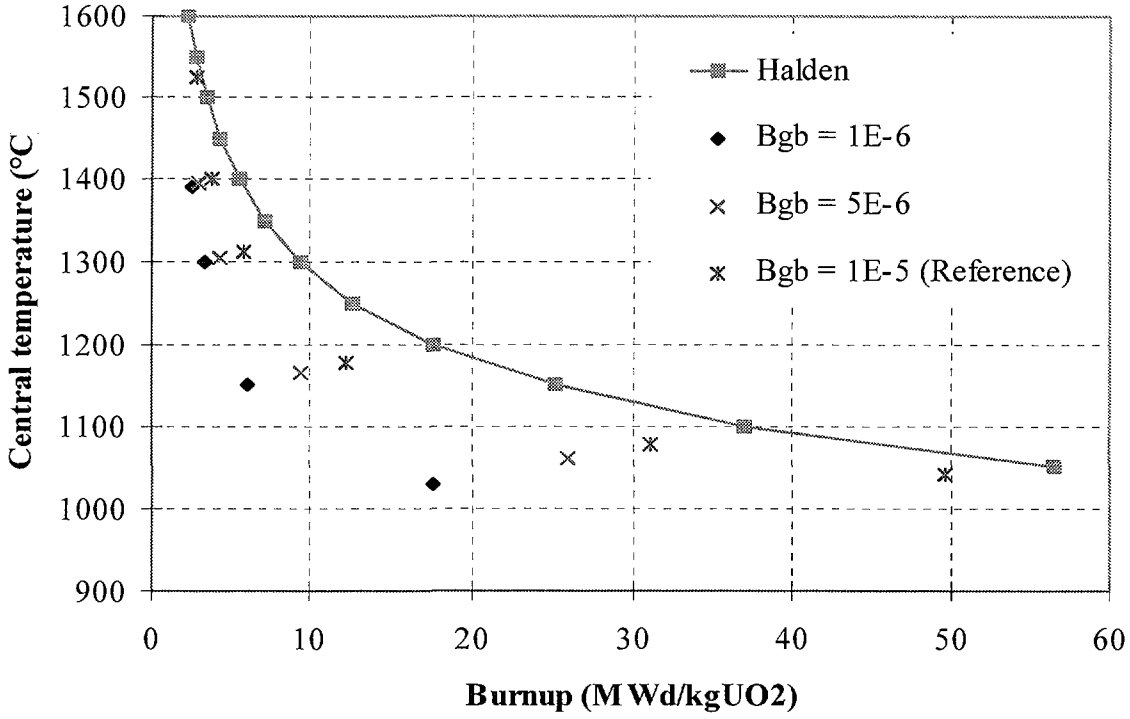

FIG. 5: The effect of resolution rate constant at the grain boundary for 20 kW/m (B_{gb}^{ref}) on the central temperature for 1% average fission gas release versus burnup during irradiation at constant linear heat rate.

3.2. Simulation of the Simplified Fumex Cases

3.2.1. Test procedure

In a second step of testing the model we have simulated the two simplified FUMEX cases [3]. Given the absence of any experimental data, the two cases enable an intercomparison with other model predictions along with testing the sensitivity to changes in experimental variables as well as the stability of the calculation. Case 1 consisted of a fuel rod running at a constant power of 20 kW/m to a final burnup of 50 MWd/kgUO_2. In the second case, the power was held constant at 20 kW/m to a burnup of 30 MWd/kgUO_2 when there was a ramp to 40 kW/m in half an hour. This high power was held to an end-of-life (EOL) burnup of 50 MWd/kgUO_2. In both cases, we have considered an uncertainty of 5% on the linear heat generating rate of the fuel rods. The general fuel rod characteristics used in the calculations are summarised in Table .

3.2.2. Results and discussion

The results for the first simplified FUMEX case are summarised in T. At end-of-life the mean central temperature prediction of the codes in the FUMEX exercise was 980.4 °C with a standard deviation of ± 110.5 °C. The fission gas release predictions at the end-of-life were typically less than 3%, with many codes predicting a release of less than 1%, that is below the

Halden empirical threshold. Our code also predicts a low fraction of released fission gases, which is in accordance with the relatively low central temperature. The results in T also highlight the rather limited sensitivity to the linear heat rate as well as the good convergence of the program.

The results for the second simplified FUMEX case are summarised in Table 3. . The mean and standard deviation of the predicted temperatures by the codes in the FUMEX exercise were 911 °C ± 78 °C before ramp, 1620 °C ± 73 °C after ramp, and 1845 °C ± 193 °C at end-of-life. The temperatures obtained by means of the FTEMP2 code (cf. Table 3.) were slightly lower but still within the error margins.

Table 1. Main parameters for the simplified FUMEX case calculations

Parameter	value	unit
pellet inside diameter	0	mm
pellet outside diameter	10.67	mm
cladding inside diameter	10.90	mm
cladding outside diameter	12.78	mm
dishing	-	-
plenum volume	2.5	cm^3
fuel column length	20	cm
fuel density	95	% TD
grain size	15	µm
enrichment U^{235}	10	%
fuel surface roughness	3	µm
clad surface roughness	1	µm
fill gas	He	-
fill gas pressure	5	bar

Table 2. Main results from the simulation of the first simplified FUMEX case

Case 1	$T_{c,EOL}$ (°C)	FGR_{EOL} (%)
nominal	900	0.42
+5% LHR	944	0.45
-5% LHR	859	0.40

Table 3. Main results from the simulation of the second simplified FUMEX case

Case 2	$T_{c,1}$ (°C)	FGR_1 (%)	$T_{c,2}$ (°C)	FGR_2 (%)	$T_{c,3}$ (°C)	FGR_3 (%)
nominal	850	0.36	1535	12.69	1693	30.95
+ 5% LHR	886	0.39	1619	14.89	1802	35.25
- 5% LHR	815	0.33	1455	9.89	1584	25.74

$_1$: before ramp
$_2$: after ramp
$_3$: at end-of-life

The majority of the codes predict a low release ≤1% before the ramp, an increase to ≈20% at 31 MWd/kgUO_2 following the ramp and a mean end-of-life FGR of 35 % with a standard deviation of ±8.2% (Three code results have been omitted in view of their unexplained extreme values). Our results are thus in good accordance with the mean values. In addition, they indicate that the fission gas release is diffusion-controlled during the high power irradiation. However, shortly after the ramp we predict slightly lower values for the fission gas release (10-15%) in comparison with the other codes (20%). There are a few factors which could affect the release kinetics during a ramp and which have to be investigated more thoroughly before drawing definite conclusions: the tube conductivity (V_t^0), the sigmoidal functions $f(\phi)$ and $g(\sigma_e)$, the hydrostatic pressure, the intraganular bubble behaviour which affects the effective volume diffusion coefficient, the resolution rate at the grain boundary bubbles, etc. However, these values can only be fine-tuned when the model for fission gas release will be coupled with an integral fuel performance code (e.g. COMETHE developed by BELGONUCLEAIRE), which is the next step of our validation process. Another contributing factor to the underprediction of the release during the ramp could also stem from the slightly lower central temperature predictions (Table 3.) and from the fact that fuel restructuring (e.g. grain growth) is disregarded in the present FGR model.

4. CONCLUSIONS AND FUTURE WORK

We have developed a new mechanistic model for fission gas release in LWR fuel. The model embodies a large number of the underlying basic mechanisms of fission gas release and it couples the kinetics of the intra- and intergranular behaviour of the gas atoms.

In a first step of the validation we have simulated the empirical Halden criterion, relating fuel central temperature to burnup at which 1% release can be exceeded, which is extremely difficult to predict accurately [3]. The general tendency of the fission gas release model is very satisfactory, more precisely it predicts the decrease of the incubation period with burnup under stationary conditions quite well. In addition, the predicted concentration of the grain boundaries at which saturation occurs is in the order of $2x10^{15}$ atoms/cm^2 which corresponds with other data in the literature [9][40].

The parametric simulation of the empirical threshold for fission gas release revealed the most important parameters for further calibration of the FGR model, namely the resolution rate at grain boundary bubbles (B_{gb}) and the hydrostatic pressure in the fuel pellet (P_h). The average grain size on the other hand does not affect the release threshold. It does however affect the release rate after interlinkage of the grain boundary bubbles occurred.

The simulation of the two simplified cases in the FUMEX round robin exercise were also satisfactory, if it wasn't for the slightly underpredicted release kinetics during the ramp in the second case. Nevertheless, before drawing definite conclusions, it is necessary to include a few improvements:

(a) obtain the fission rate, the temperature and the burnup distribution in a pellet from an integral fuel performance code (e.g. COMETHE);
(b) the hydrostatic pressure should also be accounted for since it appears to play an important role, both in the threshold for release as in the release kinetics after interlinkage occurred;

(c) we should analyse the interconnection of grain boundary bubbles by means of percolation theory in order to justify the sigmoidal curves $f(\phi)$ and $g(\sigma_e)$ provided by Kogai [17];

(d) we should reduce the calculation time in order to be able to incorporate the model in a general fuel performance code.

ACKNOWLEDGEMENTS

The author wishes to express his gratitude Dr. M. Lippens (S.A. BELGONUCLEAIRE) and Dr. M. Verwerft (SCK•CEN) for the valuable discussions and their interest in the work.

Nomenclature

δ_{gb}	=	grain boundary thickness (= 0.5 nm)
D_m^v	=	vacancy diffusion coefficient on grain boundary
Ω	=	atomic volume (= 4.09 10^{-29} m^3)
P_h	=	hydrostatic pressure around the bubble
γ	=	surface tension of the intergranular bubble
θ	=	dihedral angle between the intergranular bubble and the grain boundary (= 50°)
ρ_{bl}	=	grain boundary bubble radius of curvature
R_{bl}	=	grain boundary bubble radius in the grain face ($R_{bl} = \rho_{bl} \sin\theta$)
C_{bl}^0	=	initial concentration of intergranular bubbles (= $10^{12}/m^2$)
C_{bl}	=	concentration of intergranular bubbles
S_{gb}	=	specific surface of the grain boundaries
k	=	index corresponding to the origin of the grain (e.g. UO_2 or PuO_2 grain)
l	=	index corresponding to the grain size
m	=	index corresponding to the macroscopic annulus in which the grain is embedded
N_{klm}	=	number of grains of type k,l,m per unit of volume
R_{klm}	=	radius of the grains of type k,l,m
D_{klm}	=	volume diffusion coefficient of the fission product in the grain of type k,l,m
ζ^2	=	hard sphere diameter of the gas (= 4.047 10^{-10} m)
a	=	tube radius of interconnected grain boundary bubbles
L	=	tube length of interconnected grain boundary bubbles
b	=	resolution rate at intragranular bubbles
g	=	capture rate at intragranular bubbles
B_{gb}	=	resolution rate at intergranular bubbles
δ_R	=	half width of the zone adjacent to the grain faces where gas atoms are re-dissolved from grain boundary bubbles (= 22nm)
R	=	gas constant (= 8.314 J/mole/K)
N_A	=	number of Avogadro (= 6.02310^{23} /mole)
σ_e	=	the sum of the hydrostatic pressure (compressive) imposed on the pellet σ and the bubble pressure P_{bl} (tensile)
Y_{FP}	=	cumulative yield of fission gas atoms Xe and Kr (= 0.25)
ϕ^*	=	0.78 ($\approx \pi/4$)
σ_e^*	=	10 MPa
V_t^0	=	(2/3)*10^{-12} μm^3

REFERENCES

[1] K. UNE, S. KASHIBE, "Fission gas release during post irradiation annealing of BWR fuels", J. Nucl. Sc. and Techn. 27 (11) (1990) 1002.

[2] C. FORAT, P. BLANPAIN, B. KAPUSTA, P. GUEDENEY, P. PERMEZEL, "Fission gas release enhancement at extended burnup: experimental evidence from French PWR irradiation", IAEA-TECDOC-697, 68–75, 1992.

[3] INTERNATIONAL ATOMIC ENERGY AGENCY, "Fuel modelling at extended burnup", IAEA-TECDOC-998, 1998.

[4] P. VAN UFFELEN, "An overview of fission product release mechanisms", SCK•CEN Report R-3144, 1997.

[5] P. VAN UFFELEN, "Developments of a new fission gas release and fuel swelling model", Enlarged Halden Programme Group meeting, Lillehammer (Norway), 1998, HPR-349.

[6] U.M. EL-SAIED, D.R. OLANDER, "Fission gas release during grain growth", J. Nucl. Mat. 207 (1993) 313–326.

[7] D.R.OLANDER, "Combined grain-boundary and lattice diffusion in fine-grained ceramics", Advances in Ceramics, Vol. 17 (1986) 271–293.

[8] M.V. SPEIGHT, J.A. TURNBULL, "Enhanced fission product release by grain boundary diffusion", J. Nucl. Mat. 68 (1977) 244–249.

[9] K. UNE, S. KASHIBE, "Fission gas release during post irradiation annealing of BWR fuels", J. Nucl. Sci. Techn. 27 (11), (1990) 1002–1016.

[10] R.J. WHITE, M.O. TUCKER, "A new fission gas release model", J. Nucl. Mat. 118 (1983) 1–38.

[11] R.J. WHITE, "A new mechanistic model for the calculation of fission gas release", Proceedings ANS Top. Meet. on LWR Fuel Performance, West Palm Beach, Florida (USA), April 17–21, (1994).

[12] M. MOGENSEN, C. BAGGER, C.T. WALKER, "An experimental study of the distribution of retained xenon in transient-tested UO_2 fuel", J. Nucl. Mat. 199 (1993) 85–101.

[13] C.T. WALKER, P. KNAPPIK, M. MOGENSEN, "Concerning the development of grain face bubbles and fission gas release in UO_2 fuel", J. Nucl. Mat. 160 (1988) 10–23.

[14] C.T. WALKER, M. MOGENSEN, "On the rate determining step in fission gas release from high burnup water reactor fuel during power transients", J. Nucl. Mat. 149 (1987) 121–131.

[15] M.O. TUCKER, "Grain boundary porosity and gas release in irradiated UO_2", Rad. Eff. 53 (1980) 251–256.

[16] P. VAN UFFELEN, "Assessing the contribution of grain boundary diffusion to fission gas release in nuclear fuel", Enlarged Halden Programme Group meeting, Loen (Norway), 1999.

[17] T.KOGAI, "Modelling fission gas release and gaseous swelling of light water reactor fuels" J. Nucl. Mat. 244 (1997) 131–140.

[18] P. VAN UFFELEN, "Modelling precipitation of fission products at grain boundaries in nuclear fuel" submitted to J. Nucl. Mat., 1999.

[19] T.J. BJORLO, E. KOLSTAD, C. VITANZA, "FUEL-TEMP-2 computer programme for analysis of the steady state thermal behaviour of oxide fuel rods", HPR-211, March 1977.

[20] HILLERT, "On the theory of normal and abnormal grain growth", Acta Metallurgica, 13 (1965) 227.
[21] C. RONCHI, P.T. ELTON, "Radiation re-solution of fission gas in uranium dioxide and carbide", J. Nucl. Mat. 140 (1986) 228–244.
[22] D.R. OLANDER, "Fundamental aspects of nuclear reactor fuel elements", TID-26711-P1 (1976).
[23] A. DENIS, R. PIOTRKOWSKI, "Simulation of isothermal fission gas release", J. Nucl. Mat. 229 (1996) 149–154.
[24] M.V. SPEIGHT, "A calculation on the migration of fission gas in material exhibiting precipitation and re-solution of gas atoms under irradiation", Nucl. Sci. Eng. 37 (1969) 180–185.
[25] J.A. TURNBULL, "A review of irradiation induced re-solution in oxide fuels", Rad. Eff. 83 (1980) 243–250.
[26] R. HARGREAVES, D.A. COLLINS "A quantitative model for fission gas release and swelling in irradiated uranium dioxide", J. BR. Nucl. Energy Soc., Vol 15. No. 4 (1976) 311–318.
[27] D.M. DOWLING, R.J. WHITE, M.O. TUCKER, "The effect of irradiation-induced re-solution on fission gas release", J. Nucl. Mat. 110 (1982) 37–46.
[28] L. LANDAU, E. LIFCHITZ, "Phyique Théorique. Mécanique des fluides", Chap. 2, MIR, 1971.
[29] S. KASHIBE, K. UNE, "Effect of external restraint on bubble swelling in UO_2 fuels", Enlarged Halden Programme Group meeting, Lillehammer (Norway), 1998, HPR-349.
[30] M.V. SPEIGHT, W. BEERE, "Vacancy potential and void growth on grain boundaries", Metal Science 9 (1975) 190–191.
[31] M.S. YANG, J.R. WEERTMAN, "A test of grain boundary void growth theories by small angle neutron scattering", Scripta Metallurgica 18 (1984) 543–548.
[32] J.R. MATTHEWS, M.H. WOOD, "A simple operational gas release and swelling model II. Grain boundary gas", J. Nucl. Mat. 91 (1980) 241–256.
[33] M.R. HAYNS, M.W. FINNIS, "The response of grain boundary cavities to stress and temperature changes under conditions of continuous gas generation", Nucl. Sc. Techn. 1 (1979) 255–260.
[34] H. ZIMMERMANN, "Investigations on swelling and fission gas behaviour in uranium dioxide", J. Nucl. Mat. 75 (1978) 154–161.
[35] P. KNUDSEN, C. BAGGER, M. MOGENSEN, H. TOFTEGAARD, "Fission gas release and fuel temperature during power transients in water reactor fuel at extended burnup", IAEA-TECDOC-697, 1993, 25–31.
[36] M. MOGENSEN, C. BAGGER, H. TOFTEGAARD, P. KNUDSEN, "Fission gas release below 20 kW/m in transient tested water reactor fuel at extended burnup", IAEA-TECDOC-697, 1993, 32–37.
[37] R. MANZEL, R.P. BODMER, G. BART, "Fission gas release in high burnup fuel", IAEA-TECDOC-697, 1993, 63–67.
[38] T. KOGAI, K. ITO, Y. IWANO, "The effect of cladding restraint on fission gas release behaviour", J. Nucl. Mat. 158 (1988) 64–70.
[39] NAKAMURA, M. SUZUKI, H. UETSUKA, "Re-irradiation tests of LWR spent fuel at JMTR", Enlarged Halden Programme Group meeting, Loen (Norway), 1999.
[40] J.A. TURNBULL, "An assessment of fission gas release and the effect of microstructure at high burnup", Halden Work Report HWR-604, 1999.